

Classification of Odours with Mobile Robots Based on Transient Response

Marco Trincavelli, Silvia Coradeschi and Amy Loutfi

Abstract—Classification of odours with an array of gas sensors mounted on a mobile robot is a challenging and still relatively unexplored topic. Mobile robots able to classify an odour could navigate to a specific source or isolate high concentration areas in applications such as environmental monitoring. A key aspect to classification is to be able to process the data collected while moving the robot and using a simple and compact sensor system. In order to achieve this, we present a classification algorithm that is based on the transient response from the sensors. An analysis of how classification results vary with regards to the movement of the robot is provided and subsequently the experimental validations show that the classification performance depends more on how the robot traverses the odour plume and the quality of the transient than on the distance from the source location. The experimental validation has been done in a large unmodified indoor environment.

I. INTRODUCTION

The use of olfaction in mobile robots offers a wide potential of applications ranging from environmental monitoring to rescue robotics. Inspired by these applications, the work done in mobile olfaction has dealt with odour source localization, plume tracking, and gas distribution mapping. An important facet within these subtopics is the classification problem, that discriminates one odourant or gas source from another. However, the classification of odours using mobile robots has received little attention and most experimental validation consider a single source where algorithms for steering the movement of the robot are directly coupled to the amplitude of the sensor response.

Although the odour classification problem has been extensively addressed in static and non-robotic systems, the methods used are not necessarily directly applicable to the mobile robotics. One important restriction is due to the sampling process where many static systems use a three phase sampling, first exposing the sensor array to a reference gas and then to a target gas for a period of 30-120 seconds. Analysis of the result is then based on the steady response of the sensor. A similar approach on a mobile robot would require that the robot stops each time an odour sample were to be collected. Furthermore, the mechanism needed for a three phase sampling normally requires a hardware load (pumps, valves) that is used to flush the sensing array and force the response to a recovery before the intake of a new sample. Such a system is impractical for a mobile platform because of power consumption and weight constraints, and an open sensing array is preferable. Although, in previous

work [1] it has been shown that collecting a three phase response is feasible, overcoming these restrictions would be better suited for practical robotic applications.

In this paper we focus on how successful classification performance can be achieved when the robot is continuously moving in a large and unmodified indoor environment (approx $40 m^2$). In order for this to be possible, the presented classification algorithm uses a novel approach which considers the transient response of the gas sensors to identify different odour characters. Furthermore, an important contribution of this work lies in the assessment of the classification performance with particular consideration of the movement of the robot. Here, we examine how classification performance is affected depending on factors such as the distance from the source, the motion of the robot with respect to the odour plume, etc. To the authors knowledge such an in depth analysis of the classification performance related to mobile olfaction has not been previously performed.

II. RELATED WORKS

The challenge of odour classification with a mobile robot as it moves either towards or away from an odour source is that the concentration of an odourant is not constant. Also given the latency present in the sensor response prior to a steady state, it is not possible to rely on the power law to deduce the concentration as presented in [2]. Here, it is reasonable to assume that while the robot is moving and current concentration values are unknown, the sensors are in a state of transition. Identification of an odour using only the transient information in a signal, has been addressed previously for a number of static electronic nose systems [3], [4], [5]. Of these methods, discrete wavelet transform (DWT) applied to the transient has shown to improve the classification of a signal that also includes steady state and recovery information and to training signals consisting only of transients.

As mentioned, the classification problem in mobile olfaction has received little attention, however a handful of works have explicitly dealt with classification primarily in the context of odour based navigation and gas distribution mapping. Martinez et al. developed a system able to navigate to a specific gas source in the presence of multiple sources [6]. A biologically inspired approach using the steady state value for classification was adopted. Loutfi et al. have considered the problem of gas distribution mapping in presence of multiple gas sources emitting different odors [7]. Here the transient response was used, however, the primary performance measure was based on the accuracy of the gas

AASS Mobile Robotics Lab Örebro University, Örebro, Sweden
firstname.lastname@aass.oru.se

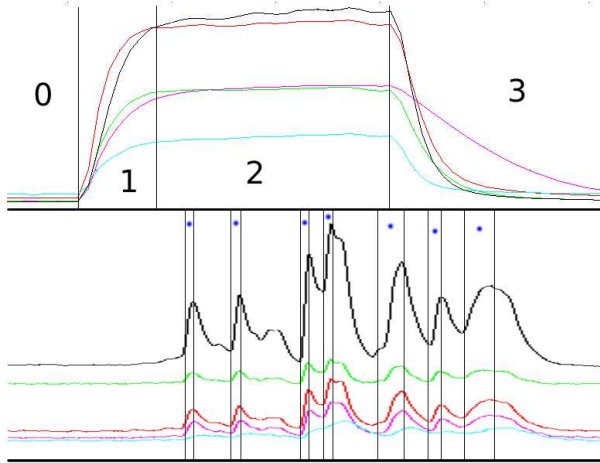


Fig. 1. Upper: example of signal collected using the traditional three phases sampling process. The phases of the sampling have been numbered in the following way: 0 baseline, 1 transient, 2 steady state, 3 recovery. Lower: example of signal collected with the mobile robot in an uncontrolled environment. The segmented transients are indicated between the bars with an asterisk.

distribution map rather than the performance of the classification algorithm. Although these works have demonstrated the feasibility of classification on mobile robots, the classification problem per se has not yet been studied in mobile olfaction. The benefit of such a study would clearly overlap into various directions of mobile robotics olfaction, namely plume tracking, gas source declaration and gas distribution mapping particularly for use in real scenarios [8].

III. CLASSIFICATION OF ODORS USING TRANSIENT RESPONSE

In order to depict the difference between a static sampling procedure and a mobile one, Figure 1 compares the readings collected from a traditional three phase sampling process and from an electronic nose which continuously samples as the robot moves (or sweeps) in the environment. In the lower part of Figure 1 the turbulence of the air flow and the uneven distribution of the gas are reflected in the signal response and in most cases, a steady state is not reached. The first step is to segment the signal and isolate the samples which represent a reaction to an odourant. Once the transient is isolated, feature extraction, data normalization and finally classification algorithms are performed.

A. Segmentation and Baseline Substraction

First a baseline subtraction is performed in order to minimize the effect of temperature, humidity and short-term drift. The baseline is given in Figure 1 as the first initial samples where the robot is stationary and is exposed only to clean air (prior to sweeping).

$$X_{n,s} = R_{n,s} - R_{o,s} \quad (1)$$

where $R_{n,s}$ is the n^{th} reading for sensor s and $R_{o,s}$ is the mean value of the baseline response.

In order to segment the transient response from the signals collected from the robot, we consider the first derivative of the signal ds/dt , for each gas sensor, s , and characterize three phases of the sensor response as:

- Baseline when $|ds/dt| < \epsilon$
- Rising phase when $ds/dt > \epsilon$
- Decay phase when $-ds/dt < \epsilon$

where ϵ is a heuristic threshold to discard smaller changes in the signal due to random oscillation in the sensor response. According to [9] the most information relevant for discrimination is present in the rising and the steady state phase. Since we can not assume that our sensors reach a steady state phase we consider only the transients in the rising phase and each segmented transient is represented by:

$$T_{t,s} = [X_{n,s} \dots X_{n+m,s}] \quad (2)$$

for $T = 1 \dots t$ transients with $X_{n,s}$ representing the first value of transient and $X_{n+m,s}$ the last value of the segmented transient.

B. Feature Extraction

As previously discussed in [3], [4], [5] classification using transient responses has mainly focused on two different feature extraction techniques namely, the Discrete Fourier Transform (DFT) and the Discrete Wavelet Transform (DWT) [10], [11]. The Discrete Fourier Transform provides a description of the signal in the frequency domain, under the assumption that the properties of the signal do not vary much during the time interval (stationary signal). The Discrete Wavelet transform instead produces a description of the signal in the time-scale domain and is therefore able to capture abrupt changes in the dynamic of the signal. The DWT is a multilevel decomposition technique that describes a signal in terms of approximation and detail coefficients calculated for different scales of a generating function called a mother wavelet. The DWT can be seen as a generalization of the DFT since the mother wavelet, in contraposition to the sine function, is not a periodical function and therefore preserves also the location in time of the frequencies it models. Therefore the DWT provides a representation that is richer but less compact than the DFT. Since it is not clear which of the two methods is best suited to the response from the gas sensors, both DWT and DFT are computed for each segmented transient and fed into the classification algorithm. A comparison of the feature extraction method with respect to the classification performance is given in Section V.

We collect the DFT or DWT for each transient response in a feature vector represented as:

$$F_i = [D_{i,1} \dots D_{i,s}] \quad (3)$$

for $1 \dots I$ transients with $D_{i,s}$ representing either the DWT or the DFT for sensor s in transient i .

C. Data Normalization

The data normalization step is aimed at smoothing the sample to sample variations, providing a more regular input to the classification module. The transformation applied is vector auto-scaling that is described by the following equations:

$$\phi_n(m) = \frac{F_n(m) - \mu_n}{\sigma_n} \quad \forall m, n \quad (4)$$

$$\text{with} \quad \mu_n = \frac{1}{M} \sum_{m=1}^M F_n(m) \quad (5)$$

$$\text{and} \quad \sigma_n = \sqrt{\frac{1}{M} \sum_{m=1}^M (F_n(m) - \mu_n)^2} \quad (6)$$

where $F_n(m)$ is the value of feature m for sample n and $\phi_n(m)$ is the normalized value of feature m for sample n . N is the total number of samples and M is the dimensionality of the feature vector. After this normalization every sample has a feature vector with zero mean and unit variance.

D. Classification

The classification model we used is the Relevance Vector Machine (RVM) introduced in [12]. This has a number of advantages over the more commonly used Support Vector Machine (SVM) since a rejection class can be defined. In other words, the output of the RVM represents posterior probabilities instead of binary or crisp decisions as in the case of the SVM. Furthermore, the extension to the multi-class case in the RVM is more principled than for the SVM [12]. In our experiments, this is important since we cannot be sure that the policy for signal segmentation is optimized for transient extraction. Therefore, by using a classifier which also provides a confidence measure we are able to tune it in such a way that transients with no definitive membership are discarded. Said differently, when the maximum of the posterior probability of a classified sample belonging to a class is too low then the transient is discarded. According to:

$$L_x = \begin{cases} \underset{k}{\operatorname{argmax}} P(C_k|x) & \text{if } P(C_k|x) \geq \Gamma \\ \text{rejected} & \text{if } P(C_k|x) < \Gamma \end{cases} \quad (7)$$

where L_x is the output label of the classifier for input vector x and $P(C_k|x)$ is the posterior probability of class k for input vector x . Γ is the rejection threshold.

Although in the presented experiments, computation is done offline, an additional advantages of using the RVM is a fast computation time during the testing phase which is suitable for mobile robot platforms with eventual real time requirements and limited computational power.

IV. EXPERIMENTAL VALIDATION

In the following experimental validation, a number of key issues are addressed:

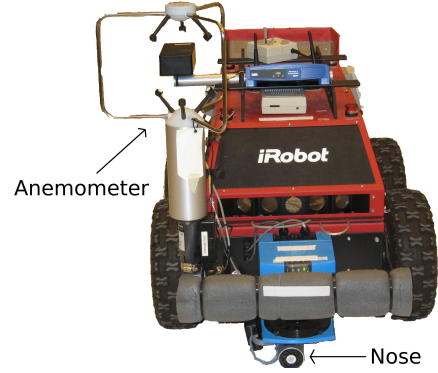


Fig. 2. The mobile robot used in the experimental validation.

- How the general classification performance using transient response varies with respect to the different feature extraction methods, namely the DFT feature extraction vs. DWT feature extraction.
- How classification performance varies depending on the movement of the robot with respect to an odour plume.
- How classification performance varies with respect to distance from the odour source location.
- Which characteristics of the transient response are the most significant for classification. Do transient responses with large amplitudes necessarily provide better classification? Also, which part of the transient response is the most critical for classification (e.g. readings which are closer to the baseline vs readings closer to a potential steady state).

A. Experimental Setup

The robot used in our experimental evaluation is shown in Figure 2. The robot was equipped with an electronic nose, an ultrasonic anemometer and a laser scanner. The nose is an array of five semiconductor gas sensors inserted in an aluminum tube with a fan at one extremity. The purpose of the fan is to provide a constant airflow to the sensors and therefore limit the influence of the movement of the robot, a summary of the gas sensors used is given in Table I. Considering the fact that the substances we chose for the experiments are heavier than air, whose molecular weight is in average 29 g/mol, the nose was mounted in horizontal position at 10 cm height on the ground, below the laser scanner. The anemometer used to measure the airflow is a Young 81000 Ultrasonic Anemometer and has a resolution of 1 cm/s and a range from 2 cm/s to 40 m/s. Its placement has been a compromise between the need for a measurement of the airflow as close as possible to the nose and to have the measurement as unaffected as possible by the body of the robot. The robot software is based on the Player server [13] that provides easy access to the sensors and the actuators. Moreover Player provides many high level algorithms such as adaptive Montecarlo localization, wavefront path-planner and vector field histogram obstacle avoidance that were used respectively for localization, global and local path planning.

Model	Gases Detected	Quantity
Figaro TGS 2600	Hydrogen, Carbon Monoxide	2
Figaro TGS 2602	Ammonia, Hydrogen Sulfide, VOC (volatile organic compound)	1
Figaro TGS 2611	Methane	1
Figaro TGS 2620	Organic Solvents	1

TABLE I
GAS SENSORS USED IN THE ELECTRONIC NOSE.

The experiments have been carried out in a large room (approx. 40 m²) with no openings. No artificial airflow has been induced. The robot was moving following a predefined sweeping trajectory covering an area of roughly 15 m². The experiment run has been repeated, executing the sweep with two different orientations: horizontal and vertical (in order to investigate the effects of different path-planning strategies on the classification performances). The gas source was a cup placed on the floor adjacent to the area covered by the movement of the robot. Figures 3 and 4 provide a graphical representation of the configuration of the experiment together with an example of the two paths followed by the robot.

The three substances considered in these experiments are ethanol, acetone and isopropyl. In Table II we report their chemical formulas and their molecular weight.

Substance	Chemical Formula	Molar Mass
Ethanol	C_2H_5OH	46 g/mol
Acetone	CH_3COCH_3	58 g/mol
Isopropyl	C_3H_8O	60 g/mol

TABLE II
LIST OF SUBSTANCES CONSIDERED IN THE EXPERIMENTS

V. RESULTS

The experiment run has been repeated 30 times, 15 with horizontal orientation and 15 with vertical orientation. The total number of transients collected is 425. We observed an airflow with direction N-E and average speed of 6 cm/s. From this fact and from the locations of the responses of the gas sensors we assume that the gas propagates as a plume according to the direction of the wind¹. Figure 3 and 4 show two example runs in which the region of the plume can be confirmed by the position of the detected transients (indicated by the circles in Figure 3) along the robot path.

A. General Classification Performance

To examine the classification performance, we perform a leave-one-out cross validation. The results are shown in Figure 5. This graph displays the classification error rate and the rejection rate for different values of the rejection threshold. We can observe how the error rate decreases for increasing rejection thresholds. This means that the calculation of the posterior probabilities is meaningful since raising the rejection threshold we discard more erroneously classified

¹This assumption is made as it is difficult to visualize the gas and thus confirm the shape of the plume

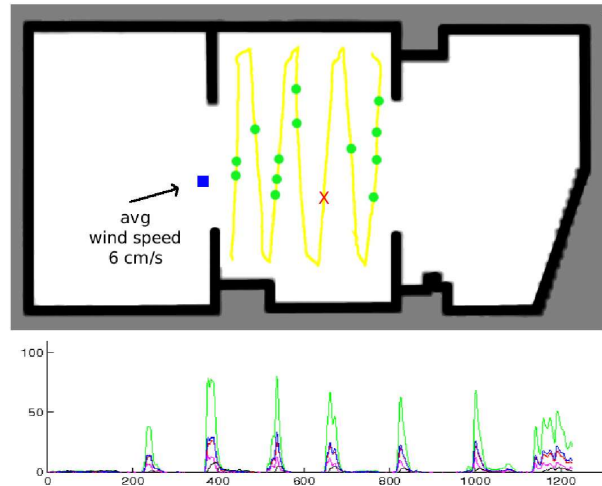


Fig. 3. Upper: Example of experiment in which the analyte was isopropyl. The robot follows a horizontal sweeping trajectory frequently entering and exiting the plume. The arrow shows the average direction and magnitude of the windflow. The square indicates the position of the source. The solid line is the trajectory of the robot. The circles and crosses are locations in which we obtained a transient that could be classified at a rejection threshold of 0.8. The circles represent correctly classified transients, while the crosses represent the incorrectly classified transients. Lower: The actual sensor readings collected during the run.

samples than correct ones. Another important observation is that the DWT based features clearly outperform the FFT based ones. A lower classification error is obtained for every rejection threshold maintaining approximately the same rejection rate.

Table III reports the confusion matrix for the DWT-based classifier when the rejection threshold is set to zero, and therefore no sample is rejected. Here, the ethanol and isopropyl are more difficult to discriminate than the acetone.

B. Classification Depending on Sweeping Strategy

Figure 6 reports the results of leave-one-out cross validation for the DWT based classifier dividing the samples according to the sweep orientation. For rejection thresholds greater than 0.8 the vertical sweeping obtains a better classification accuracy despite a higher rejection rate. Figure 3 and 4 give us more insight on the characteristics of the signal we collect in the two sweeping modalities. It is evident from the sensor readings that performing the path displayed in Figure 3 the robot crosses the plume, allowing the sensors to recover completely in between one branch of the sweep and the next. On the other hand, in Figure 4 the robot stays in the plume for longer time and the sensors almost never go back to the baseline level until the end of the experiment. Interestingly, while many odour source localization strategies isolate source location by following a plume and thus traversing its width, for a classification application it is most likely better to remain inside the plume as long as possible to optimize classification performance. It should be noted that assumptions about the shape and direction of the plume have been made based on wind direction [14] and sensors response.

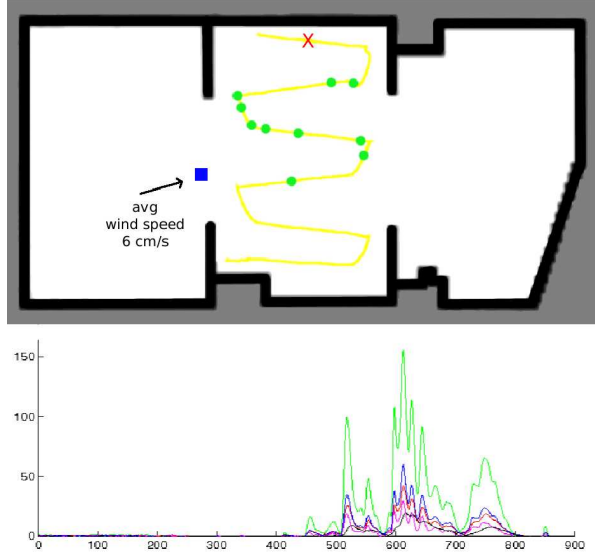


Fig. 4. Upper: Example of experiment in which the analyte was ethanol. The robot follows a vertical sweeping trajectory and remains continuously in the plume. The arrow shows the average direction and magnitude of the windflow. The square indicates the position of the source. The solid line is the trajectory of the robot. The circles and crosses are locations in which we obtained a transient that could be classified at a rejection threshold of 0.8. The circles represent correctly classified transients, while the crosses represent the incorrectly classified transients. Lower: The actual sensor readings collected during the run.

	Ethanol	Aceton	Isopropyl
Ethanol	133	0	13
Aceton	1	150	1
Isopropyl	27	0	100

TABLE III

CONFUSION MATRIX OF THE RVM CLASSIFIER WITH A ZERO REJECTION RATE. THE COLUMNS INDICATE THE CORRECT CLASSES, WHILE THE ROWS REFER TO THE ESTIMATED CLASSES.

C. Classification Performance w.r.t. Distance to the Source

Figure 7 shows a scatterplot of the positions in which sensor responses have been obtained and classified for various rejection thresholds. The triangles which indicate misclassified transients are distributed equally in the inspected area, indicating that proximity to the source does not necessarily guarantee good classification performance. Also, it is worth noting that correctly classified transients, indicated by dots, were still obtained at a distance of 4-5 meters from the source location.

D. Classification Performance w.r.t Transient Characteristics

In order to gain insight into how the characteristics of the transient affect classification performance, two measures γ and η are extracted. These measures are defined as

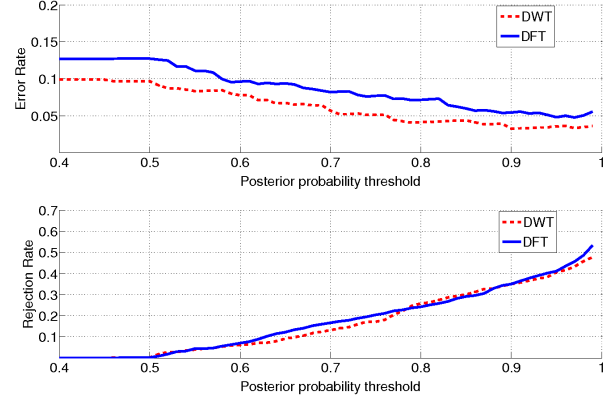


Fig. 5. Classification and rejection rate of the classifier with a varying rejection threshold. The dashed line represents a classifier trained with DWT based features, while the solid line represents a classifier trained with FFT based features.

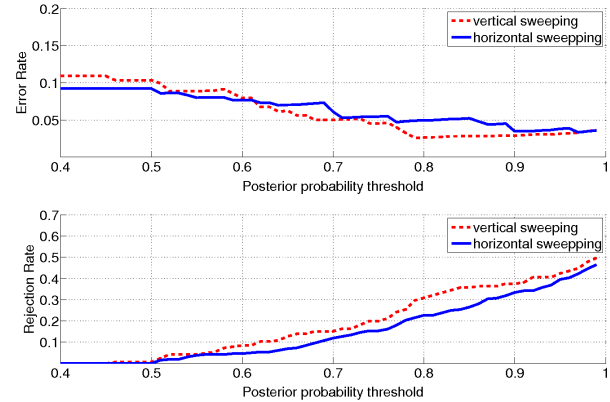


Fig. 6. Comparison of the classification results obtained with respect to the moving strategy of the robot.

$$\gamma = \frac{\sum_{t=1}^N \mu_n}{N} \quad (8)$$

$$\eta = \max \mu_n - \min \mu_n \quad \text{where} \quad (9)$$

$$\mu_n = \frac{\sum_{s=1}^S X_{n,s}}{S} \quad (10)$$

The first measure γ captures the distance of the transient from the baseline response. Here, μ_t represents the mean of all the values of all sensors at reading n for a particular transient. N is the total number of readings in a transient and S is the total number of sensors. The second measure η is based on the amplitude of the transients calculated by the difference of the minimum and the maximum value of μ_n .

Therefore in Figure 8 the histogram can be used to depict the correct classifications (seen on the left-hand figure) and incorrect classification (right), with the value of γ on the x-axis. Here, incorrect classifications primarily occur on transients close to the baseline (i.e. lower mean values).

In Figure 9 a histogram is used to depict the correct classifications and incorrect classifications with value η shown on the x-axis. Transients which have higher amplitudes, where the sensors have had longer exposure to an odour,

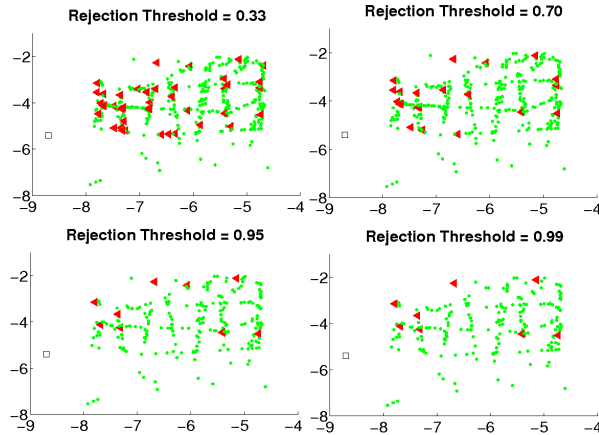


Fig. 7. Scatterplot of the positions of the classified samples. The square indicates the position of the gas source, the circles indicate correct classifications and the triangles indicate incorrect classifications. The distances reported on the axis are in meters.

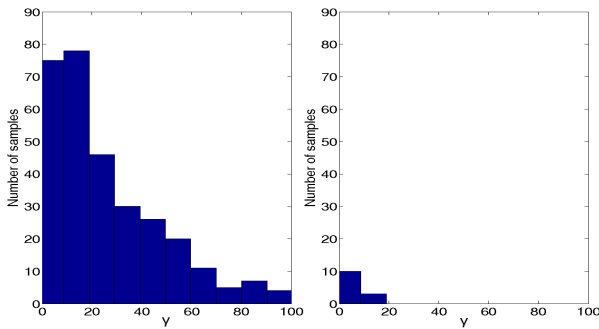


Fig. 8. Left: The histogram of the correctly classified samples with respect to γ . Right: The histogram of the incorrectly classified samples with respect to γ .

are classified correctly. For example, in Figure 4 at sample 600 a number of transients occur far from the baseline while in Figure 3 almost all transients begin at the baseline values. Comparing these two figures, higher classification success is more likely to be achieved in Figure 4. Combining these two results we can see that errors are concentrated in transients which have a small amplitude and are close to the baseline. To achieve good classification, we prefer either a transient with high amplitude or smaller transients that occur in sequence after one another without a complete recovery. It is important to note that these results are validated with the assumption that only one gas is present. Nonetheless, these results suggest that it worth optimizing a path planning algorithm in order to collect higher quality data with respect to classification.

VI. CONCLUSIONS AND FUTURE WORKS

The results presented in this paper are an important step-forward in making mobile olfactory robots applicable for realistic environments. In particular, the data processing methods allow the robot to move continuously while collecting and analyzing odour samples, therefore are suitable to be used in odour based navigation as well as gas dis-

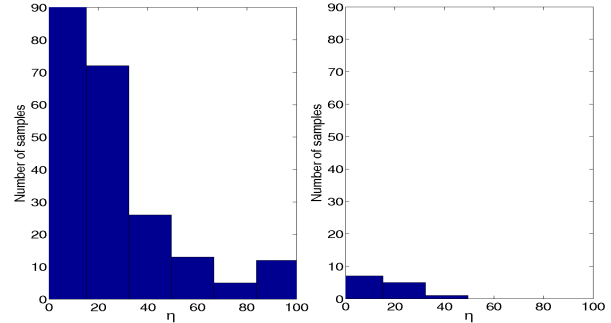


Fig. 9. Left: The histogram of the correctly classified samples with respect to η . Right: The histogram of the incorrectly classified samples with respect to η .

tribution mapping applications. By analyzing the classification performance in terms of the movement of the robot, better autonomous navigation strategies can be developed. An important point to consider is to gather insight into the properties of an odor plume using the wind information provided by the anemometer. These will be the primary directions for future works. In addition, future work will also analyze the classification problem when dealing with odour mixtures.

REFERENCES

- [1] A. Loutfi and S. Coradeschi, "Smell, Think and Act: A Cognitive Robot Discriminating Odours," *Autonomous Robots*, vol. 20, no. 3, pp. 231–238, 2006.
- [2] O. Rochel, D. Martinez, E. Hugues, and F. Sarry, "Stereo-olfaction with a sniffing neuromorphic robot using spiking neurons," in *16th European Conference on Solid-State Transducers - EUROSENSORS, Prague, Czech Republic*, Sept. 2002.
- [3] R. Gutierrez-Osuna, A. Gutierrez-Galvez, and N. U. Powar, "Transient response analysis for temperature modulated chemoresistors," *Sensors and Actuators B: Chemical B*, vol. 93, no. 1-3, pp. 57–66, 2003.
- [4] C. Distanto, M. Leo, P. Siciliano, and K. Persaud, "On the study of feature extraction methods for an electronic nose," *Sensors and Actuators B*, vol. 87, pp. 274–288, 2002.
- [5] L. Marques, U. Nunes, and A. de Almeida, "Olfaction-based mobile robot navigation," *Thin Solid Films*, vol. 418, pp. 51–58, 2002.
- [6] D. Martinez, O. Rochel, and E. Hughes, "A biomimetic robot for tracking specific odors in turbulent plumes," *Autonomous Robots*, vol. 20, pp. 185–195(11), June 2006.
- [7] A. Loutfi, S. Coradeschi, A. J. Lilienthal, and J. Gonzalez, "Gas distribution mapping of multiple odour sources using a mobile robot," *Robotica*, *Accepted*, vol. 20, 2008.
- [8] A. J. Lilienthal, A. Loutfi, and T. Duckett, "Airborne chemical sensing with mobile robots," *Sensors*, vol. 6, pp. 1616–1678, October 2006.
- [9] R. Gutierrez-Osuna, H. T. Nagle, and S. S. Schiffman, "Transient response analysis of an electronic nose using multi-exponential models," *Sensors and Actuators B*, vol. 61, pp. 626–632, 1999.
- [10] P. Duhamel and M. Vetterli, "Fast fourier transforms: A tutorial review and a state of the art," *Signal Processing*, vol. 19, pp. 259–299, 1990.
- [11] S. Mallat, *A wavelet tour of signal processing*. Academic Press, 1998.
- [12] M. E. Tipping, "Sparse bayesian learning and the relevance vector machine," *Journal of Machine Learning Research*, vol. 1, pp. 211–244, 2001.
- [13] B. Gerkey, R. T. Vaughan, and A. Howard, "The Player/Stage Project: Tools for Multi-Robot and Distributed Sensor Systems," in *Proceedings of the IEEE International Conference on Advanced Robotics (ICAR)*, 2003, pp. 317–323.
- [14] H. Ishida, "Robotic systems for gas/odor source localization: Gap between experiments and real-life situations," in *Proceedings of the IEEE International Conference on Intelligent Robots and Systems, 2005. (IROS 2005)*, 2007, pp. 3–8.